ESIPT of 1-[N-(2-pyridyl) aminomethylidene]-2(1H)-Naphtalenone: A TDDFT study

Dapeng Yang[a,b]*, Rui Zheng[a], Yusheng Wang[a], and Jian Lv[a]

[a] *College of Mathematics and Information Science, North China University of Water Resources and Electric Power, Zhengzhou 450045, China*
[b] *State Key Laboratory of Molecular Reaction Dynamics, Theoretical and Computational Chemistry, Dalian Institute of Chemical Physics, Chinese Academy of Sciences, Dalian 116023, China*

Abstract. In the present work, the excited state intramolecular proton transfer (ESIPT) process between the Enol and Keto forms of the title compound has been investigated with the time-dependent density functional theory (TDDFT) method. The geometric structures, frontier molecular orbitals, electrostatic potential (ESP) maps as well as the absorption and fluorescence spectra of the two forms of the title compound have been investigated. The calculated absorption spectra of the Keto form are more in agreement with the experimental results. Moreover, the potential energy curves of the intramolecular proton transfer (IPT) within the title compound have been scanned in both ground state S_0 and the first excited state S_1. We found that the intramolecular proton transfer from Enol form to Keto form in excited state is almost barrierless with an energy barrier 2.1 kJ/mol whereas intramolecular proton transfer between the two forms of the title compound in ground state is forbidden with energy barrier as high as 10.5 kJ/mol.
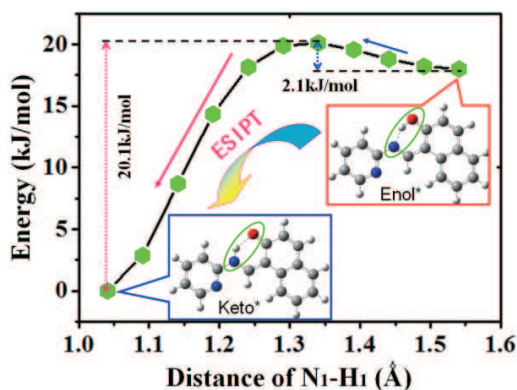
*Corresponding author. *Email address:* dpyang_ncwu@163.com (D.-P. Yang)

1   Introduction

As one of the most important weak interactions, hydrogen bonding plays important roles in organometallic molecules, crystal packing of many organic, nucleic acids, stabilization of the secondary structure of biomolecules like proteins, and so forth [1-4]. Its significance is conspicuous in various real life examples and a thorough investigations of hydrogen bonding interactions will be vital to delve into the critical evaluation of many phenomenon coming up not only in the crystal state, but also in solutions and living organisms [5-6]. Zhao and Han have determined that intermolecular hydrogen bonding between solute and solvent molecules should be significantly strengthened in the corresponding electronic excited states after photo-excitation theoretically [7-12], since which many investigations of mechanism involved in exited state hydrogen bonding need to be revisited in physics, chemistry and biology. Up to now, many different sensing mechanisms, such as intramolecular charge transfer (ICT), photo-induced electron transfer (PET), fluorescence resonance energy transfer (FRET), and excited state proton transfer (ESPT) and so forth [13-21], are relevant with hydrogen bonding. Particularly, the excited state inter- and intra- molecular proton transfer (ESIPT) reactions have been drawing great attention due to their unique photo-physical and photo-chemical properties. Many novel optoelectronic applications, such as molecular switches, fluorescence sensors, UV filters, laser dyes and LEDs and so forth [22-29], are facilitated based on ESIPT reactions. Naturally, the attention focused on this phenomenon is both cognitive and applied, through which it crops up as a demanding subject of research even today.

1-[N-(2-pyridyl) aminomethylidene]-2(1H)-Naphtalenone, as one of the Schiff base compounds, displays interesting photochromic and thermochromic features [30-40]. Photochromism arise via H-atom transfer from the hydroxy O atom to the imine N atom [30, 31]. Such proton-exchanging materials can be utilized for the design of various molecular electronic devices [32-34]. In general, 2-hydroxy Schiff bases display two possible tautomeric forms, the enol-imine (OH) and the keto-amine (NH) forms. Depending on the tautomers, two types of intramolecular hydrogen bonds are observed in Schiff bases: O-H$\cdots$N in enol-imine and N-H$\cdots$O in keto-amine tautomers [34-38], as shown in Scheme 1. In previous publication, IR, ^{1}H NMR, ^{13}C NMR, UV-vis and the crystal structure of the title compound had been studied [39]. Also some physicochemical properties of the title compound had been investigated using the DFT method [40]. However, to the best of our knowledge, geometric optimizations of the excited-state structures as well as theoretical calculations of the emission spectra of the title compound have not been carried out yet.

Moreover, there are almost no available literatures about the intramolecular proton transfer process within the title compound. Therefore, in the present work, the excited-state molecular structures, emission spectra and the S_0 and S_1 potential energy surfaces of the intramolecular proton transfer of the title Schiff base compound have been investigated using the TDDFT/B3LYP/6-31+G(d, p) method with salvation model IEFPCM. Theoretically predicted values were compared with the experimentally measured data and the results were discussed.

Scheme 1: The schematic structures of the Enol and Keto forms of the title compound.
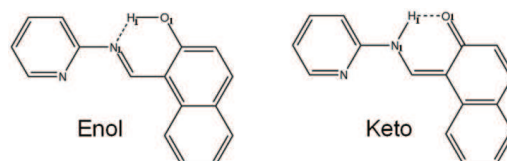
2   Computational details

In the present work, all electronic structure calculations were accomplished based on the Gaussian 09 program suite [41]. The geometric optimizations of the two forms of the title compound were performed using DFT in the S_0 state and using TDDFT in the S_1 state. During all the electronic structure calculations, Becke's three-parameter hybrid exchange functional with Lee-Yang-Parr gradient-corrected correlation (B3LYP functional) was used [42, 43]. Other two range-separated functionals LC-BLYP and CAM-B3LYP, which even though have been shown to be efficient in reproducing the excitation energies [44, 45] and HOMO-LUMO gaps [46, 47], is not suitable for the title compound. Basis set 6-31+G(d, p) is used throughout all the calculations, which is an appropriate basis set for the system. Solvation effects were included using the integral equation formalism [48, 49] (IEF) version of the polarizable continuum [50, 51] (PCM) model with the dielectric constant of chloroform (ε=4.7113). All the local minima were confirmed by the absence of an imaginary mode in the vibrational analyses. No constrains for symmetry, bonds, angles or dihedral angles were applied in the geometric optimization calculations. The S_0 and S_1 potential energy surfaces of the intramolecular proton transfer have been scanned by constrained optimizations and frequency analyses to obtain the thermodynamic corrections in their corresponding electronic states, and keeping the N_1-H_1 bond length fixed at a series of values.

3   Results and discussion

3.1   Geometric structures in states S_0 and S_1

Fig. 1 shows the optimized geometric structures of the Enol and Keto forms of the title compound in both states S_0 and S_1 at the IEFPCM-TDDFT/B3LYP/6-31+G(d, p) theory

Table 1: Bond lengths (Å) and dihedral angles (°) of Enol and Keto forms of the title compound in states S_0 and S_1 at IEFPCM-TDDFT/B3LYP/6-31+G(d, p) theory level.

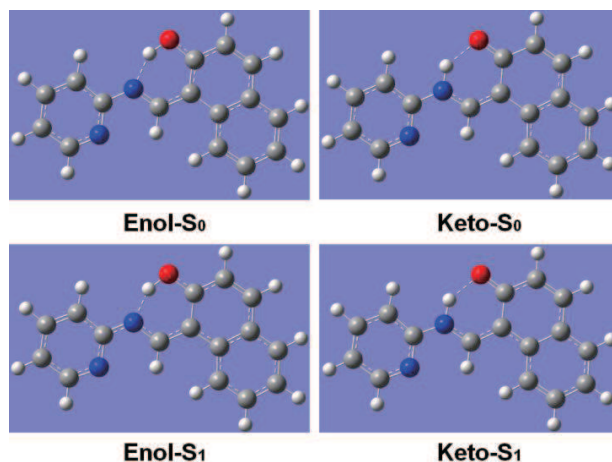|	Enol			Keto	
	S_0	S_1		S_0	S_1
$N_1 \cdots H_1$	1.613	1.541	$N_1\text{-}H_1$	1.034	1.044
$H_1\text{-}O_1$	1.016	1.043	$H_1 \cdots O_1$	1.736	1.700
$\angle N_1\text{-}H_1\text{-}O_1$	149.191	152.031	$\angle N_1\text{-}H_1\text{-}O_1$	136.657	140.256

Figure 1: Optimized geometric structures of the Enol and Keto forms of the title compound in both states S_0 and S_1 at the IEFPCM-TDDFT/B3LYP/6-31+G(d, p) theory level.

level. Corresponding bond lengths and dihedral angles are collected in Table 1. One can see that in ground state S_0, intramolecular hydrogen bonds $N_1 \cdots H_1\text{-}O_1$ and $N_1\text{-}H_1 \cdots O_1$ are formed in the Enol and Keto forms of the title compound respectively. Upon photoexcitation, the optimized geometric structures of the two forms of the title compound in excited state S_1 seem to be similar to those in the ground state. However, after checking the corresponding bond lengths and dihedral angles collected in Table 1, we found that the distance between atoms N_1 and H_1 in Enol form is shortened from 1.613 Å in ground state S_0 to 1.541 Å in excited state S_1 whereas that between atoms O_1 and H_1 in Keto form is shortened from 1.736 Å in ground state S_0 to 1.700 Å in excited state S_1. This may indicate that excited-state intramolecular proton transfer will take place from Enol form to Keto form upon photoexcitation.

3.2   Electronic spectra and frontier molecular orbitals

The electronic excitation energies as well as the oscillation strengths of the six low-lying electronically excited states for both the Enol form and the Keto form of the title compound are calculated at the TD-B3LYP/6-31+G(d, p) level of theory in both vacuo and

Table 2: The calculated electronic excitation energies (nm) and corresponding oscillator strengths of the Enol and Keto forms of the title compound at TD-DFT/B3LYP/6-31+G(d, p) theory level in both vacuo and solvent chloroform (IEFPCM). The orbital contributions of transition S_0-S_1 are also listed. Two range-separated functionals CAM-B3LYP and LC-BLYP are also used for comparisons.

	Enol					
	vacuo			IEFPCM		
	B3LYP	CAM-B3LYP	LC-BLYP	B3LYP	CAM-B3LYP	LC-BLYP
S_1	391.5 (0.4554) H→L (98%)	354.6 (0.5375) H→L (95%)	329.1 (0.5640) H→L (89%)	401.2 (0.5839) H→L (99%)	362.5 (0.6673) H→L (95%)	335.2 (0.6896) H→L (89%)
S_2	334.2	293.2	273.6	335.7	295.7	275.7
S_3	304.3	276.3	257.9	303.1	275.1	256.9
S_4	301.8	269.1	248.9	299.9	269.5	250.2
S_5	292.3	255.5	235.3	295.9	254.9	235.4
S_6	285.7	251.6	234.4	285.1	252.3	233.6
	Keto					
	vacuo			IEFPCM		
	B3LYP	CAM-B3LYP	LC-BLYP	B3LYP	CAM-B3LYP	LC-BLYP
S_1	408.1 (0.4032) H→L (99%)	373.1 (0.4693) H→L (97%)	349.0 (0.5124) H→L (92%)	419.9 (0.5138) H→L (99%)	384.2 (0.5671) H→L (97%)	359.7 (0.6012) H→L (91%)
S_2	372.3	331.1	302.4	361.9	322.5	294.6
S_3	354.6	302.5	271.7	356.6	306.6	277.2
S_4	318.7	278.1	258.9	311.2	278.4	258.5
S_5	297.1	258.6	240.4	294.6	254.6	239.3
S_6	287.4	242.8	221.8	292.1	245.1	224.5

solvent chloroform (IEFPCM) and presented in Table 2. Two range-separated functionals CAM-B3LYP and LC-BLYP are also used for comparisons. From Table 2, we can find that for both of the two forms of the title compound, the first singlet excited state S_1 corresponds to the largest oscillation strength, which indicates that both of them should be first excited to this lowest singlet excited state. For the Enol form, the S_0-S_1 excitation energies calculated at TD-DFT/B3LYP/6-31+G(d, p) theory level in vacuo and solvent chloroform (IEFPCM model) are 391.5 and 401.2 nm, respectively. The redshift should be due to the solvation effect of the chloroform. For the Keto form of the title compound, the S_0-S_1 excitation energies calculated at TD-DFT/B3LYP/6-31+G(d, p) theory level in vacuo and solvent chloroform (IEFPCM model) are 408.1 and 419.9 nm respectively, which are redshifted by approximately 20 nm relative to the corresponding values of the Enol form. For both the Enol and the Keto forms of the title compound, the other two range-separated
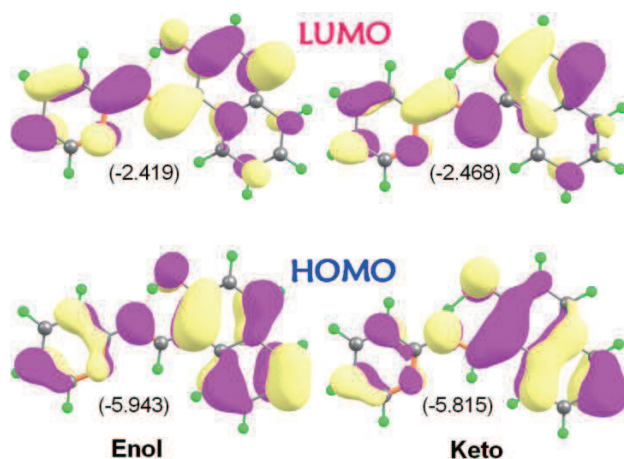
Figure 2: The shapes and energies (eV) of the frontier MOs involved in the S_0-S_1 electronic excitation of the Enol and Keto forms of the title compound at the IFPCM-TDDFT/B3LYP/6-31+G(d, p) theory level.

functionals CAM-B3LYP and LC-BLYP give much higher S_0-S_1 excitation energies.

Experimentally, the UV-vis spectrum of 2-hydroxy Schiff bases that exist mainly as Enol form indicate the presence of a band at <400 nm, whereas compounds exist as Keto form show a new band, especially in polar and nonpolar solvents, at >400 nm [52-55]. Electronic absorption spectra of the title compound in chloroform solvent show a band at 430 nm, which should be resulted from the Keto form [39] not the Enol form in chloroform solvent. Therefore, in chloroform solvent, most of the title compound should be in the Keto form and the tautomerization between Enol and Keto forms of the title compound in the ground state is impossible, which will be discussed in detail in Section 3.3.

Fig. 2 shows the shapes and energies of the frontier MOs (HOMO and LUMO) involved in the S_0-S_1 electronic excitation of the Enol and Keto forms of the title compound calculated at the IFPCM-TDDFT/B3LYP/6-31+G(d, p) theory level. For Enol form, it can be noticed that from HOMO to LUMO, the electron cloud density on atom O_1 is decreased whereas that on atom N_1 is increased, which once again predicts that intramolecular proton transfer will take place from atom O_1 to atom N_1 in the excited state. Similar changes of the electron cloud density are not observed in the Keto form of the title compound, which implies that intramolecular proton transfer from atom N_1 to atom O_1 will not happen in the excited state. The above conclusions drawn from the changes of electron cloud density from HOMO to LUMO are consistent with the discussions in the following section.

3.3   The potential energy curves and the PT mechanism

As discussed in Section 3.2, judging from the comparisons between the experimentally observed UV-vis spectra of 2-hydroxy Schiff bases [39, 52-55] and the calculated S_0-S_1
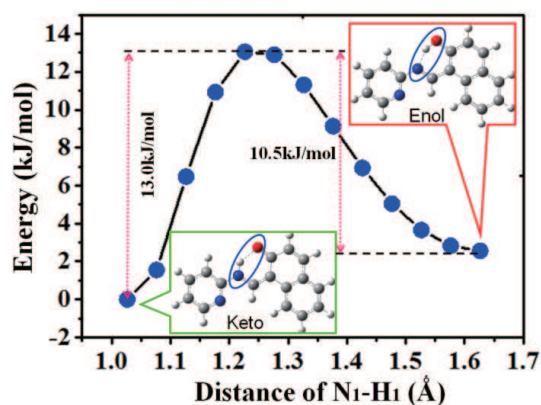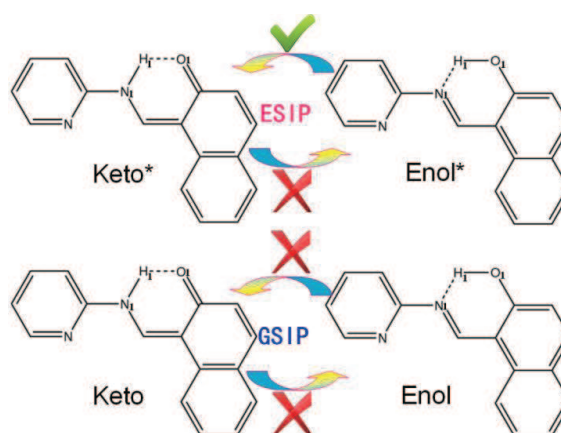
Figure 3: Scanned potential energy curve from Keto to Enol forms of the title compound along with the N_1-H_1 bond length. The insets show the detailed configuration.

excitation energies of the Enol and Keto forms of the title compound, we have concluded that in chloroform solvent, most of the title compound should be in the Keto form and the tautomerization between Enol and Keto forms of the title compound in the ground state is impossible. To further confirm this viewpoint, we have scanned the potential energy curves along with the lengthening of the distance between the N_1 and the H_1 atoms in both ground state S_0 and the first excited state S_1. Fig. 3 shows the scanned ground-state potential energy curve from Keto to Enol forms of the title compound along with the N_1-H_1 bond length. It can be found from Fig. 3 that there is an energy barrier higher than 10 kJ/mol between the two forms of the title compound. Therefore, neither the tautomerization from Keto to Enol nor the tautomerization from Enol to Keto is possible in the ground state, see Scheme 2. Moreover, the potential energy of the Keto form is 2.5 kJ/mol lower than the Enol form, which once again confirms that most of the title compound should be in the Keto form in the ground state.

Scheme 2: Schematic view of the intramolecular proton transfer between the two forms of the title compound in ground state S_0 (GSIPT) and excited state S_1 (ESIPT).
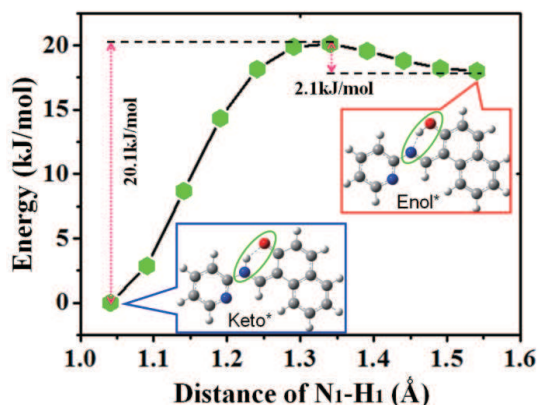
Figure 4: Scanned potential energy curve from Keto* to Enol* forms of the title compound along with the N_1-H_1 bond length. The insets show the detailed configuration.

In addition, Fig. 4 shows the scanned excited-state potential energy curve from Keto* to Enol* forms of the title compound along with the N_1-H_1 bond length. From Fig. 4, we can find that there is an energy barrier higher than 20 kJ/mol from the Keto* form to the Enol* form of the title compound. Therefore, ESIPT from N_1 to O_1 is not possible in the excited state S_1. However, from Enol* form to Keto* form, the energy barrier is just 2.1 kJ/mol, which is almost barrierless. Moreover, the potential energy of the Keto* form is 18 kJ/mol lower than that of the Enol* form, which will efficiently facilitate the ESIPT from O_1 to N_1 in excited state S_1. Therefore, tautomerization from Enol* to Keto* is quite possible in the excited state S_1, see Scheme 2.

4 Conclusion

In the present work, we have investigated the excited-state intramolecular proton transfer (ESIPT) process between the Enol and Keto forms of the title compound with the time-dependent density functional theory (TDDFT) method at the IEFPCM-B3LYP/6-31+G(d, p) level. The calculated absorption spectra of the Keto form are more in agreement with the experimental results than the Enol form. The potential energy curves of the intramolecular proton transfer (IPT) within the title compound have been scanned in both ground state S_0 and the first excited state S_1. We found that the intramolecular proton transfer from Enol* form to Keto* form in excited state is almost barrierless with an energy barrier 2.1 kJ/mol whereas intramolecular proton transfer between the two forms of the title compound in ground state is forbidden with an energy barrier as high as 10.5 kJ/mol.

References

[1] S. Scheiner, Hydrogen Bonding: A Theoretical Perspective, Oxford University Press, New York, 1997.

[2] I. Alkorta, I. Rozas, J. Elguero, Chem. Soc. Rev. 27 (1998) 163.

[3] G. R. Desiraju, T. Steiner, The weak hydrogen bond: In structural chemistry and biology, Oxford University Press, Oxford, 1999.

[4] G. Gilli, P. Gilli, J. Mol. Struct. 552 (2000) 1.

[5] L. Sobczyk, S. J. Grabowski, T. M. Krygowski, Chem. Rev. 105 (2005) 3513.

[6] S. J. Grabowski, Chem Rev. 111 (2011) 2597.

[7] G. J. Zhao, K. L. Han, J. Phys. Chem. A. 111 (2007) 2469.

[8] G. J. Zhao, K. L. Han, J. Comput. Chem. 29 (2008) 2010.

[9] S. Chai, G. J. Zhao, P. Song, S. Q. Yang, J. Y. Liu, K. L. Han, Phys. Chem. Chem. Phys. 11 (2009) 4385.

[10] G. J. Zhao, K. L. Han, Phys. Chem. Chem. Phys. 12 (2010) 8914.

[11] G. J. Zhao, B. H. Northrop, P. J. Stang, K. L. Han, J. Phys. Chem. A. 114 (2010) 3418.

[12] G. J. Zhao, K. L. Han, Acc. Chem. Res. 45 (2012) 404.

[13] Y. H. Liu, M. S. Mehata, J. Y. Liu, J. Phys. Chem. A. 115 (2011) 19.

[14] P. W. Zhou, J. Y. Liu, S. Q. Yang, J. S. Chen, K. L. Han, G. Z. He, Phys. Chem. Chem. Phys. 14 (2012) 15191.

[15] P. Song, F. C. Ma, Int. Rev. Phys. Chem. 32 (2013) 589.

[16] D. P. Yang, Y. Zhang, Spectrochimica Acta Part A. 131 (2014) 214.

[17] P. Zhou, J. Y. Liu, K. L. Han, G. Z. He, J. Comput. Chem. 35 (2014) 109.

[18] D. P. Yang, Y. G. Yang, Y. F. Liu, Spectrochimica Acta Part A. 117 (2014) 379.

[19] J. F. Zhao, H. B. Yao, J. Y. Liu, M. R. Hoffmann, J. Phys. Chem. A. 119 (2015) 681.

[20] J. F. Zhao, J. S. Chen, Y. L. Cui, J. Wang, L. X. Xia, Y. M. Dai, P. Song F. C. Ma, Phys. Chem. Chem. Phys. 17 (2015) 1142.

[21] J. F. Zhao, J. S. Chen, J. Y. Liu, M. R. Hoffmann, Phys. Chem. Chem. Phys. 17 (2015) 11990.

[22] P. T. Chou, M. L. Martinez, W. C. Cooper, C. P. Chang, Appl. Spectrosc. 48 (1994) 604.

[23] A. Kawanabe, Y. Furutani, K. H. Jung, H. Kandori, J. Am. Chem. Soc. 131 (2009) 16439.

[24] J. Keck, H. E. A. Kramer, H. Port, T. Hirsch, P. Fischer, G. Rytz, J. Phys. Chem. 100 (1996) 14468.

[25] T. G. Kim, Y. Kim, D. J. Jang, J. Phys. Chem. A. 105 (2001) 4328.

[26] L. M. Tolbert, K. M. Solntsev, Acc. Chem. Res. 35 (2002) 19.

[27] O. Poizat, E. Bardez, G. Buntinx, V. Alain, J. Phys. Chem. A. 108 (2004) 1873.

[28] G. Jung, S. Gerharz, A. Schmitt, Phys. Chem. Chem. Phys, 11 (2009) 1416.

[29] Y. Kubo, S. Maeda, S. Tokita, M. Kubo, Nature. 382 (1996) 522.

[30] E. Hadjoudis, M. Vitterakis, I. M. Mavridis, Tetrahedron 43 (1987) 1345.

[31] X. X. Xu, X. Z. You, Z. F. Sun, X. Wang, H. X. Liu, Acta Crystallogr. C 50 (1994) 1169.

[32] L. Feringa, W. F. Jager, B. De Lange, Tetrahedron 49 (1993) 8267.

[33] I. Willner, S. Rubin, Angew. Chem. Int. Ed. Engl. 35 (1996) 367.

[34] M. Yavuz, H. Tanak, J. Mol. Struct.: Thermochem. 961 (2010) 9.

[35] A. A. Agar, H. Tanak, M. Yavuz, Mol. Phys. 108 (2010) 1759.

[36] A. Ozek, C. Albayrak, M. Odabasoglu, O. Büyükgüngör, Acta Cryst. C63 (2007) o177.

[37] H. Ünver, M. Kabak, D. Mehmet Zengin, T. Nuri Durlu, J. Chem. Crystallogr. 31 (2001) 203.

[38] H. Tanak, F. Ersahin, Y. Köysal, E. Agar, S. Isik, M. Yavuz, J. Mol. Mod. 15 (2009) 1281.

[39] T. Hökelek, Z. Kılıç, M. Isiklan, M. Toy, J. Mol. Struct. 523 (2000) 61.

[40] M. Toy, H. Tanak, J. Theo, Comput. Chem. 11 (2012) 745.

[41] M. J. Frisch, G. W. Trucks, H. B. Schlegel, G. E. Scuseria, M. A. Robb, J. R.; Scalmani, G. Cheeseman, V. Barone, B. Mennucci, G. A. Petersson, H. Nakatsuji, M. Caricato, X. Li, H. P. Hratchian, A. F. Izmaylov, J. Bloino, G. Zheng, J. L. Sonnenberg, M. Hada, M. Ehara, K. Toyota, R. Fukuda, J. Hasegawa, M. Ishida, T. Nakajima, Y. Honda, O. Kitao, H. Nakai, T. Vreven, J. A. Montgomery, Jr. J. E. Peralta, F. Ogliaro, M. Bearpark, J. J. Heyd, E. Brothers, K. N. Kudin, V. N. Staroverov, R. Kobayashi, J. Normand, K. Raghavachari, A. Rendell, J. C. Burant, S. S. Iyengar, J. Tomasi, M. Cossi, N. Rega, J. M. Millam, M. Klene, J. E. Knox, J. B. Cross, V. Bakken, C. Adamo, J. Jaramillo, R. Gomperts, R. E. Stratmann, O. Yazyev, A. J. Austin, R. Cammi, C. Pomelli, J. W. Ochterski, R. L. Martin, K. Morokuma, V. G. Zakrzewski, G. A. Voth, P. Salvador, J. Dannenberg, S. Dapprich, A. D. Daniels, O. Farkas, J. B. Foresman, J. V. Ortiz, J. Cioslowski, D. J. Fox, Gaussian 09, Revision A.02; Gaussian, Inc.: Wallingford, CT, 2009.

[42] S. H. Vosko, L. Wilk, M. Nusair, Can. J. Phys 58 (1980) 1200.

[43] C. Lee, W. Yang, R. G. Parr, Phys. Rev. B. 37 (1988) 785.

[44] B. M. Wong, M. Piacenza, F. D. Sala, Phys. Chem. Chem. Phys. 11 (2009) 4498.

[45] M. P. Balanay, D. H. Kim, J. Phys. Chem. 115 (2011) 19424.

[46] M. J. G. Peach, E. I. Tellgren, P. Sałek, T. Helgaker, D. J. Tozer, J. Phys. Chem. A 111 (2007) 11930.

[47] B. M. Wong, T, H. Hsieh, J. Chem. Theory Comput. 6 (2010) 3704.

[48] E. Cances, B. Mennucci, J. Tomasi, J. Chem. Phys. 107 (1997) 3032.

[49] B. Mennucci, E. Cances, J. Tomasi, J. Phys. Chem. B, 101 (1997) 10506.

[50] S. Miertus, E. Scrocco, J. Tomasi, Chem. Phys. 55 (1981) 117.

[51] R. Cammi, J. Tomasi, J. Comput. Chem. 16 (1995) 1449.

[52] H. Unver, M. Yildiz, D. M. Zengin, S. Ozbey, E. Kendi, J. Chem. Crystallogr. 31 (2001) 211.

[53] H. Tanak, A. Agar, M. Yavuz, Int. J. Quant. Chem. 111 (2011) 2123.

[54] S.R. Salman, F. S. Kamounah, Spectrosc. Lett. 35 (2002) 327.

[55] M. Yildiz, Z. Kilic, T. Hokelek, J. Mol. Struct. 441 (1998) 1.